

# Representations of faces and body parts in macaque temporal cortex: A functional MRI study

Mark A. Pinsk\*<sup>†</sup>, Kevin DeSimone\*<sup>†</sup>, Tirin Moore<sup>§</sup>, Charles G. Gross\*, and Sabine Kastner\*<sup>†</sup>

\*Department of Psychology and <sup>†</sup>Center for the Study of Brain, Mind, and Behavior, Princeton University, Green Hall, Princeton, NJ 08544; and <sup>§</sup>Department of Neurobiology, Stanford University School of Medicine, Sherman Fairchild Building, Stanford, CA 94305

Contributed by Charles G. Gross, March 30, 2005

**Human neuroimaging studies suggest that areas in temporal cortex respond preferentially to certain biologically relevant stimulus categories such as faces and bodies. Single-cell studies in monkeys have reported cells in inferior temporal cortex that respond selectively to faces, hands, and bodies but provide little evidence of large clusters of category-specific cells that would form “areas.” We probed the category selectivity of macaque temporal cortex for representations of monkey faces and monkey body parts relative to man-made objects using functional MRI in animals trained to fixate. Two face-selective areas were activated bilaterally in the posterior and anterior superior temporal sulcus exhibiting different degrees of category selectivity. The posterior face area was more extensively activated in the right hemisphere than in the left hemisphere. Immediately adjacent to the face areas, regions were activated bilaterally responding preferentially to body parts. Our findings suggest a category-selective organization for faces and body parts in macaque temporal cortex.**

non-human primate | visual category representations

**H**uman and non-human primates have a remarkable ability to recognize a large variety of different objects in their environments. In humans, neuroimaging studies have shown that object information is represented in a large swath of ventral temporal and lateral occipital cortex that is characterized by stronger responses to objects than to non-objects (1, 2). Within these object-selective activations, discrete regions have been identified that respond preferentially to some biologically relevant stimulus categories such as faces [the “fusiform face area,” FFA (3–6)] or bodies [the “extrastriate body area,” EBA (7)], suggesting a category-specific and anatomically segregated modular organization of neural representations related to certain classes of object stimuli. These studies are consistent with reports of patients with lesions of temporoccipital cortex, who show selective impairments in recognizing familiar faces [prosopagnosia (8)] or body parts (9) but not other objects.

In the macaque, much less is known about the large-scale representation of object information. Single-cell physiology studies have shown that neurons in inferior temporal (IT) cortex typically respond to complex stimuli with some selectivity for shape, color, and texture (10, 11). A small proportion of IT neurons were found to respond selectively to faces (10–16), hands (14, 17), or human bodies (18). These neurons were more common in the portion of cytoarchitectonic area TE on the ventral bank of the superior temporal sulcus (STS) and in the superior polysensory area on the dorsal bank of the STS. They were also found on the lateral and ventral surfaces of area TE. Even though face-selective neurons were found clustered together, or sometimes even formed columns (19, 20), there was no evidence for an organization into face- or body-selective areas in monkey IT cortex, similar to the human FFA or EBA.

However, this view has recently been challenged by the demonstration of discrete face-selective areas in the posterior and anterior STS by using functional MRI (fMRI) in anesthetized and awake macaques (21, 22). The face-selective areas were embedded in a large object-selective activation extending from

area V4 to rostral TE (22). These studies were the first to provide evidence of category-selective areas in monkey IT cortex. Here, we probe the neural representations of two classes of biologically relevant stimuli, monkey faces and body parts, using fMRI in behaving macaques.

## Methods

**Subjects.** Subjects were three adult, male macaque monkeys (*Macaca fascicularis*) weighing 4–9 kg. All procedures were approved by the Princeton University Animal Care and Use Committee and conformed to National Institutes of Health guidelines for the humane care and use of laboratory animals.

Details regarding surgery, experimental setup, data acquisition, and analysis are described by Pinsk *et al.* (23) and will only be briefly summarized here. Each animal was surgically implanted with a plastic head bolt by using ceramic screws and dental acrylic. Monkeys were placed in an MR-compatible primate chair prone with their heads erect and rigidly fixed in a head-holding apparatus. The animals were acclimated to the MRI environment through the use of a mock scanner. Monkeys were trained to fixate on a small dot at the center of a display screen by using an infrared eye-tracking system (Applied Science Laboratories, Bedford, MA). By providing the animals with regular juice rewards while they maintained fixation within a 4° square window, and systematically increasing the reward rate during the course of a trial, the animals were trained to fixate for as long as 4 min.

**Visual Stimuli and Experimental Design.** Color pictures of monkey faces, monkey body parts, and man-made objects were presented on a screen while the animals maintained fixation (see Fig. 4, which is published as supporting information on the PNAS web site). The stimuli subtended 12 × 12° and were presented for 1 s foveally behind the fixation point (0.5° diameter), followed by a 1-s blank interval during which only the fixation point was present. Several additional categories of stimuli (food, laboratory scenes) were presented during each trial, the results of which will be described in a separate report. Blocks of stimuli from each category were presented interleaved with blank periods, each lasting for 12 s. Each category block was repeated twice within a trial, resulting in trials of 240 s each. Monkey M3 was only tested for faces in relation to pictures of houses instead of man-made objects and not for body parts. Stimulus presentation and eye position recordings were synchronized to the beginning of each scan by using a trigger pulse from the scanner.

**Data Acquisition.** Structural and functional images were acquired with a 3-T head-dedicated scanner (Magnetom Allegra, Siemens, Erlangen, Germany), using a 12-cm transmit/receive surface coil (NMSC-023, Nova Medical, Wakefield, MA). For

Abbreviations: aBody, anterior body part; aFace, anterior face; EBA, extrastriate body area; FFA, fusiform face area; fMRI, functional MRI; IT, inferior temporal; pBody, posterior body part; pFace, posterior face; STS, superior temporal sulcus.

<sup>†</sup>To whom correspondence should be addressed. E-mail: mpinsk@princeton.edu.

© 2005 by The National Academy of Sciences of the USA

cortical surface reconstructions, a high-resolution ( $0.5 \times 0.5 \times 0.5$  mm) structural scan was acquired in a separate session during which the animals were anesthetized with Telazol (tiletamine/zolazepam, 10 mg/kg i.m.) [MPRAGE sequence; field of view (FOV) =  $128 \times 128$  mm;  $256 \times 256$  matrix; TR = 2,500 ms; TE = 4.4 ms; TI = 1,100 ms; flip angle =  $8^\circ$ ; 20 acquisitions]. All other scan sessions were performed with awake animals. Functional images were taken with a gradient echo, echo planar imaging sequence (FOV =  $80 \times 80$  mm;  $64 \times 64$  matrix; TR = 2,400 ms, TE = 32 ms, flip angle =  $90^\circ$ , bandwidth = 2,112 Hz per pixel). Twenty-seven contiguous coronal slices (thickness of 2 mm without gap; in-plane resolution of  $1.25 \times 1.25$  mm) were acquired in six to eight series of 100 images each, starting from the posterior pole and covering the brain up to the region of the principal sulcus. An in-plane magnetic field map image was acquired to perform echo planar imaging undistortion (FOV =  $80 \times 80$  mm;  $64 \times 64$  matrix; TR = 600 ms, TE = 8.8/11.3 ms; flip angle =  $45^\circ$ ). An anatomical scan was also acquired in the same session to facilitate cortical surface alignments ( $0.5 \times 0.5 \times 1.0$  mm, MPRAGE sequence; FOV =  $128 \times 128$  mm;  $256 \times 256$  matrix; TR = 2,500 ms; TE = 4.4 ms; TI = 1,100 ms; flip angle =  $8^\circ$ ; 1 acquisition).

In total, 4,400 and 4,800 functional volumes were acquired in monkeys M1 and M2 in a total of six scan sessions per animal. In monkey M3, 600 functional volumes were acquired in a single session. The reliability of activations was investigated in monkey M1, who repeated the experiment twice with 3,000 functional volumes acquired in five and four scan sessions, respectively.

**Data Analysis.** Data were analyzed by using AFNI (<http://afni.nimh.nih.gov/afni>), FRESURFER (<http://surfer.nmr.mgh.harvard.edu>), and SUMA (<http://afni.nimh.nih.gov/afni/suma>). Scans during which the animal broke fixation  $>20$  times and for longer than 500 ms each time were excluded from fMRI analysis. The functional images were motion-corrected to the image acquired closest to the anatomical scan, undistorted by using the field map scan (24), and spatially filtered with a 2-mm Gaussian kernel. Each time series was normalized to its mean to input all of the time series across scan sessions into a single multiple regression analysis. Square-wave functions matching the time course of the experimental design were convolved with a gamma-variate function (25) and used as regressors of interest in a multiple regression model in the framework of the general linear model (26). Additional regressors to account for variance due to baseline shifts between time series, linear drifts within time series, and head motion were included in the regression model. Brain regions responding more strongly to faces or body parts were identified by contrasting presentation blocks of faces with objects and body parts with objects, respectively, similar to definitions used in previous human fMRI studies (3, 4, 6, 27). The statistical maps were thresholded at a Z score of 2.33 ( $P < 0.01$ ) and overlaid on anatomical scans or cortical surface reconstructions.

Regions of interest within temporal cortex were defined as clusters of 10 or more contiguous voxels. Clusters smaller than 10 voxels were included as regions of interest only if a larger cluster ( $>10$  voxels) was found in the same anatomical location of the other hemisphere. The raw, unsmoothed fMRI signals were averaged across all activated voxels within a given region of interest and across scans, and normalized to the mean intensity obtained during the blank periods. Statistical significance was determined by two-sample *t* tests assuming unequal variances on the averaged peak intensities of fMRI signals for each condition obtained in a given scan session and in both monkeys. The selectivity of each area for the different stimulus categories was assessed by computing a category selectivity index [CSI =  $(R_{cat} - R_{ctrl}) / (R_{cat} + R_{ctrl})$ , where  $R_{cat}$  is the averaged response of peak MRI intensities obtained during face or body part

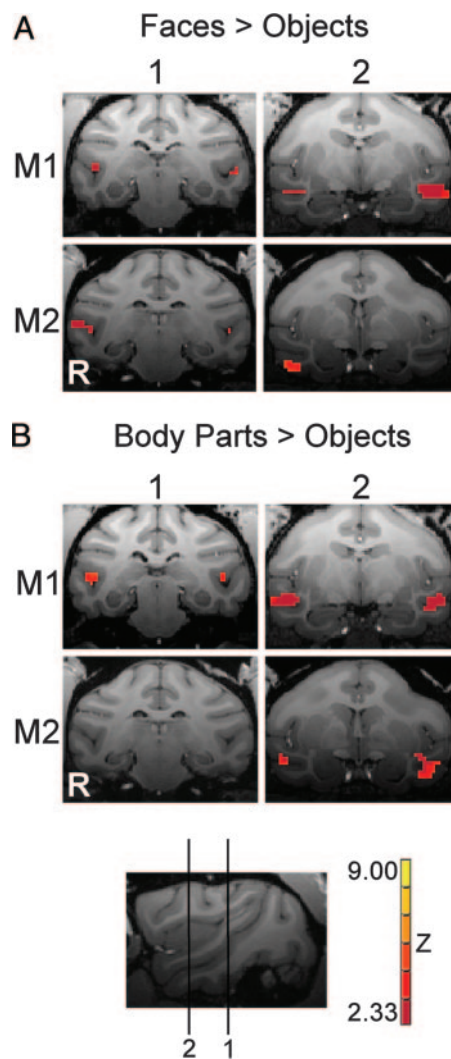


**Fig. 1.** Category-selective representations of faces and body parts in monkey temporal cortex. (A) Coronal slices of monkeys M1 and M2 depicting voxels activated significantly more by faces compared to objects. (B) Same coronal slices depicting voxels activated significantly more by body parts compared with objects. Approximate locations of the coronal slices (1, 2) are indicated on a sagittal slice. Scale indicates Z-score values of functional activity in colored regions. R, right hemisphere.

conditions and  $R_{ctrl}$  is the averaged response obtained during the object condition].

Eye-movement analysis was performed with ILAB software (28) and confirmed that the animals maintained fixation for almost all of the time during scanning sessions. For example, during a typical session, monkey M2 maintained fixation within the  $4^\circ$  window for  $97 \pm 1\%$  of the time and made an average of  $2.5 \pm 1$  eye movements outside the window that lasted for  $>500$  ms before returning to the window.

## Results

To identify brain regions that responded more strongly to faces than man-made objects, we contrasted face and object conditions and compared the resulting activations in monkeys M1–M3. This contrast revealed two activated regions in temporal cortex ( $Z > 2.33$ ,  $P < 0.01$ ). A posterior face (pFace) area was activated bilaterally along the fundus and banks of the posterior STS (slice 1 in Fig. 1A), and an anterior face (aFace) area, also activated bilaterally, was found in the anterior STS and on the

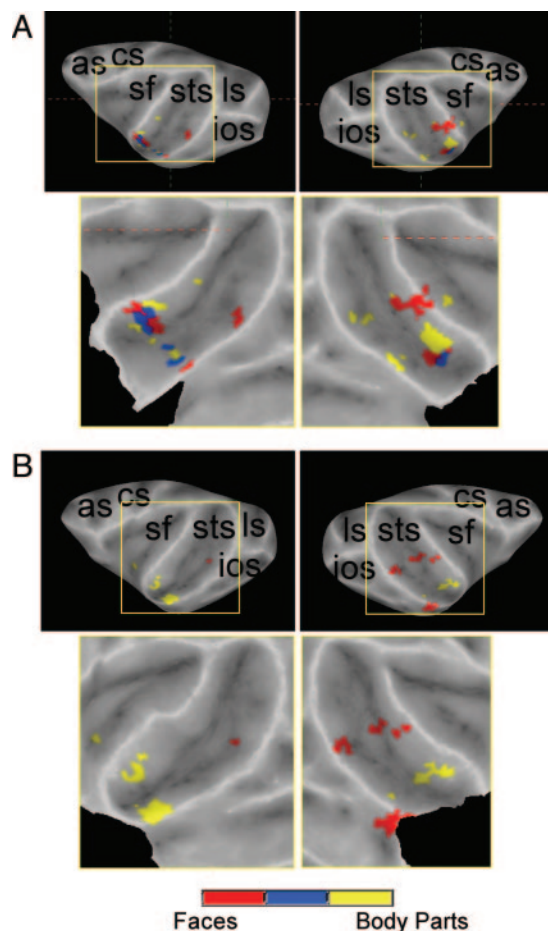


**Fig. 2.** Topographic relationship of face and body part areas. Inflated and flattened cortical surface representations of the left and right hemispheres of monkeys M1 (A) and M2 (B). Activated voxels are color-coded according to their preferred category. Faces > objects, red; body parts > objects, yellow; overlap of the two, blue. sts, superior temporal sulcus; sf, sylvian fissure; ios, inferior occipital sulcus; ots, occipitotemporal sulcus; ls, lunate sulcus; ips, inferior parietal sulcus; cs, central sulcus; as, arcuate sulcus.

middle temporal gyrus (MTG) (slice 2 in Fig. 1A). There was some variability in the locations of these areas among the three animals. For example, M1's aFace area was located on both banks and fundus of the STS, whereas M2's aFace area was located only on the right MTG (Fig. 1A). Activations in similar locations were also found in M3 (Fig. 5, which is published as supporting information on the PNAS web site).

Brain regions that responded more strongly to body parts than to man-made objects were identified by contrasting monkey body part and object conditions and comparing the resulting activity in monkeys M1 and M2. This contrast revealed two activated regions in the temporal cortex ( $Z > 2.33$ ,  $P < 0.01$ ). A posterior body part (pBody) area was found along the banks and fundus of the STS in M1 (slice 1 in Fig. 1B) but not in M2. A second region was found more anterior along the STS. This anterior body part (aBody) area was activated bilaterally in both monkeys and located on the banks and the fundus of the STS (slice 2 in Fig. 1B).

It is important to note that the differences in activation patterns could not be attributed to systematic differences in eye movements while viewing the three categories of stimuli. Fixation performance was similar for the three monkeys, and there were no significant differences in the amount of horizontal and vertical eye movements made while viewing stimuli of the three

**Table 1.** Activated volumes in category-selective areas

Monkey	Area	Activated volume, mm <sup>3</sup>	
		RH	LH
M1	pFace	56.25	12.5
	aFace	18.75	103.13
	pBody	21.88	6.25
	aBody	121.88	87.5
M2	pFace	56.25	6.25
	aFace	53.13	0
	aBody	56.25	121.88
M3*	pFace	56.25	0
	aFace	31.25	3.13
Mean $\pm$ SE	pFace	56 $\pm$ 0	6 $\pm$ 4
	aFace	34 $\pm$ 10	35 $\pm$ 34
	aBody	89 $\pm$ 33	105 $\pm$ 17

\*Face responsive regions in monkey M3 were defined in a single scan session by comparing faces to houses rather than to objects.

different categories [e.g., monkey M2: horizontal eye movements,  $F_{0.05}(2,45) = 1.16$ ,  $P = 0.32$ ; vertical eye movements,  $F_{0.05}(2,45) = 0.52$ ,  $P = 0.59$ ].

The anatomical relationship between the face and body part areas was examined by determining the responsiveness of each voxel shown in the activation maps of Fig. 1 for M1 and M2 to faces (color-coded in red), body parts (color-coded in yellow), or both stimuli (color-coded in blue). The color-coded voxels were then projected onto inflated and flattened cortical surface reconstructions (Fig. 2). With this presentation format, there appears to be a larger number of category-selective areas compared to those shown in Fig. 1. However, this is a result of the data-display procedures. When neighboring voxels touch cortically distant regions (e.g., upper and lower banks of a sulcus), they tend to separate when projected onto the cortical surface. Face-selective regions in M1 were located in the lower and upper banks of the posterior STS in the left and right hemispheres, respectively (Fig. 2A). Interestingly, the more anterior activations in M1 for faces and body parts appeared to be continuous and also partially overlapping. The body part-selective area in the anterior STS in M2 was located on both banks, and the aFace-selective area was found to be adjacent and ventral to it on the right MTG (Fig. 2B). Overall, this topography suggests a representation of the appearance of the monkey body in the anterior STS and MTG. It is possible that there is a second representation in the posterior STS, as suggested by the findings in M1, but this will need further study.

To examine the extent of the category-selective activations, the volumes of the activated regions in the left and right hemisphere were analyzed and compared in the three animals (Table 1). The size of the face activations ranged from 3 mm<sup>3</sup> to 103 mm<sup>3</sup>, and the size of the body part activations ranged from 87 mm<sup>3</sup> to 121 mm<sup>3</sup>. There were no significant differences in activated volumes between the right and left hemisphere in any of the category-selective areas except for the pFace area, which showed a larger activation volume in the right than in the left hemisphere in each of the three monkeys [ $t(2) = 13.85$ ,  $P < 0.01$ ].

The reliability of activations for the face and body part areas in the STS was examined in monkey M1, who participated in two additional experiments (Exps. 2 and 3 in Fig. 6, which is published as supporting information on the PNAS web site) that were similar to our original study (Exp. 1 in Fig. 6). Exp. 2 was identical to Exp. 1 in terms of the experimental design but involved a higher-resolution echo planar imaging sequence

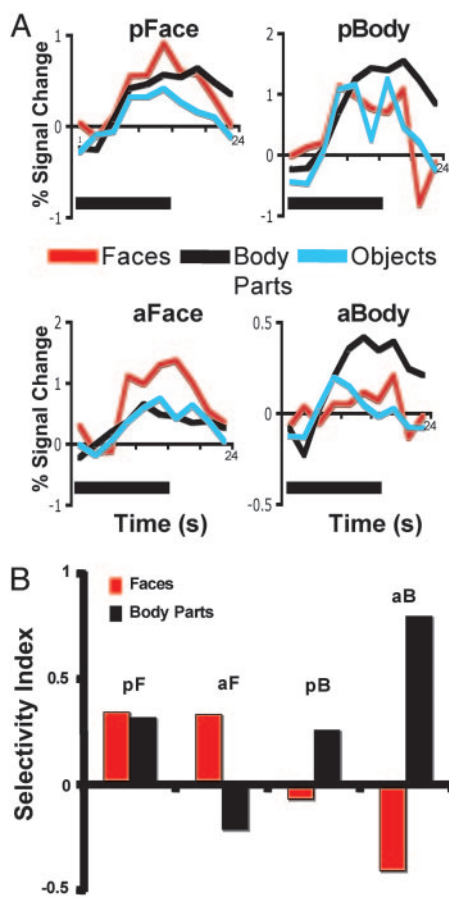


**Fig. 3.** Time courses of fMRI signals from category-selective areas. (A) Signals from the pFace, pBody, aBody, and aFace areas averaged across two monkeys (M1 and M2). The duration of the visual stimulation epoch is indicated by the black bar. The pBody area was activated only in M1. Note the y-axis scale change for the time courses in the pFace and the aBody areas. (B) Selectivity of each area to faces (red) and body parts (black) relative to objects, computed with an index (see *Methods* and *Results*).

( $1.25 \times 1.25 \times 1.25$  mm instead of  $1.25 \times 1.25 \times 2.0$  mm). In Exp. 3, we probed only the face and object, but not the body part condition. Both the pFace and the aFace areas were activated across the three experiments (Fig. 6A). Furthermore, the volume of the pFace area in the right hemisphere was larger than in the corresponding area of the left hemisphere in both additional experiments (Exp. 2:  $97 \text{ mm}^3$  vs.  $0 \text{ mm}^3$ ; Exp. 3:  $53 \text{ mm}^3$  vs.  $16 \text{ mm}^3$ ), thus replicating the right hemisphere asymmetry found across the three monkeys in Exp. 1. The aBody area, but not the pBody area, was activated in Exp. 2 (Fig. 6B), suggesting that activations of the aBody area were more robust and reliable than those of the pBody area.

The response properties and category selectivity of face- and body part-related activations were studied by performing a time course analysis of fMRI signals (Fig. 3A). fMRI signals were averaged across all activated voxels within each region, across hemispheres, scans, and monkeys M1 and M2 and normalized to the average signals obtained during blank periods. This analysis revealed that both face areas responded two to three times as strongly to faces than objects [pFace: faces vs. objects,  $t(128) = 3.20$ ,  $P < 0.01$ ; aFace: faces vs. objects,  $t(142) = 4.22$ ,  $P < 0.01$ ]. However, the pFace area was as responsive to faces as to body parts [pFace: faces vs. body parts,  $t(119) = 0.68$ , not significant], whereas body parts did not evoke significantly stronger responses than objects in the aFace area [aFace: body parts vs. objects,

$t(141) = -0.62$ , not significant] (Fig. 3A). Both the posterior and aBody areas responded more strongly to body parts than to objects and faces [pBody: body parts vs. objects,  $t(61) = 2.48$ ,  $P < 0.05$ ; body parts vs. faces,  $t(61) = 2.91$ ,  $P < 0.01$ ; aBody: body parts vs. objects,  $t(138) = 4.76$ ,  $P < 0.01$ ; body parts vs. faces,  $t(138) = 4.65$ ,  $P < 0.01$ ]. However, objects and faces both evoked a considerable and similar response in the posterior area, whereas almost no activity was elicited by these stimuli in the aBody area (Fig. 3A). The differences in category selectivity were further quantified with a category selectivity index (CSI). Values close to 1 indicate strong selectivity for a given stimulus category (faces and body parts) relative to the control category (objects). Values around 0 indicate no preference between the stimulus category and the control category. And negative values indicate a greater preference for the control category than the probed stimulus category. It is striking that the aFace and aBody areas as well as the pBody area were highly selective for faces and body parts, respectively, whereas the pFace area did not discriminate between faces and body parts (Fig. 3B and Table 2, which is published as supporting information on the PNAS web site).

## Discussion

Our results confirm previous fMRI studies reporting face-selective activations in apparently similar anatomical locations in anesthetized (21) and awake macaques (22). They extend these results by demonstrating an area responding selectively to body parts adjacent to the face-selective area in the anterior STS. In addition, our results suggest a more extensive activation of the pFace area in the right hemisphere than in the left hemisphere. The differences in activations that we obtained with face, body part, and object stimuli are unlikely to reflect differences in the attentional state of the animals performing the passive viewing task. On such an account, one would not predict reliable activations of the same regions across different experiments, high test-retest reliability in the same experiment, or consistent activations across individual monkeys, all of which were demonstrated in our study.

Neurons responding more strongly to faces than to other visual stimuli have been found, on both banks and the floor of the STS, and less prominently on the lateral and ventral convexity of IT cortex (10–16). These STS “face cells” were often found clustered together in patches and sometimes formed columns (19, 20). However, their overall proportion was reported to be small, 20% of visually responsive cells at the most (15), and no evidence for a “face area” consisting of chiefly face responsive cells was found. Indeed, bilateral lesions of the STS did not induce specific impairments in face discrimination but led only to mild impairments in discrimination of eye gaze (29, 30). Our results, on the other hand, suggest that a large proportion of neurons that are regionally clustered together in the anterior and posterior STS must be activated selectively in response to faces to evoke sufficiently strong blood oxygenation level-dependent signals. Single-cell physiology studies in animals, in which the face-selective blood oxygenation level-dependent signals will guide the electrode placement, will be necessary to address this apparent discrepancy.

In humans, functional brain imaging studies have demonstrated a distributed neural system activated specifically by faces consisting of areas in the lateral fusiform gyrus (the FFA), lateral inferior occipital gyrus, and STS (3, 31). These different areas appear to be involved in different aspects of the perceptual analysis of faces. Perception of face identity was shown to be associated with regions in the inferior occipital and fusiform gyri, and perception of eye gaze, eye, and mouth movements, and facial expressions was associated with the STS region (32–35). Our finding of several face-responsive areas exhibiting different degrees of category-selectivity raises the possibility that face



36. Hasselmo, M. E., Rolls, E. T. & Baylis, G. C. (1989) *Behav. Brain Res.* **32**, 203–218.
37. Perrett, D. I., Smith, P. A., Potter, D. D., Mistlin, A. J., Head, A. S., Milner, A. D. & Jeeves, M. A. (1985) *Proc. R. Soc. London Ser. B* **223**, 293–317.
38. Perrett, D. I., Hietanen, J. K., Oram, M. W. & Benson, P. J. (1992) *Philos. Trans. R. Soc. London B* **335**, 23–30.
39. Peelen, M. V. & Downing, P. E. (2005) *J. Neurophysiol.* **93**, 603–608.
40. Vermeire, B. A., Hamilton, C. R. & Erdmann, A. L. (1998) *Behav. Neurosci.* **112**, 1048–1061.
41. Ifune, C. K., Vermeire, B. A. & Hamilton, C. R. (1984) *Behav. Neural Biol.* **41**, 231–235.
42. Hauser, M. D. (1993) *Science* **261**, 475–477.
43. DeRenzi, E., Perani, D., Carlesimo, G. A., Silveri, M. C. & Fazio, F. (1994) *Neuropsychologia* **32**, 893–902.
44. Hilliard, R. D. (1973) *Cortex* **9**, 246–258.
45. Oram, M. W. & Perrett, D. I. (1996) *J. Neurophysiol.* **76**, 109–129.
46. Perrett, D. I., Harries, M. H., Bevan, R., Thomas, S., Benson, P. J., Mistlin, A. J., Chitty, A. J., Hietanen, J. K. & Ortega, J. E. (1989) *J. Exp. Biol.* **146**, 87–113.
47. Astafiev, S. V., Stanley, C. M., Shulman, G. L. & Corbetta, M. (2004) *Nat. Neurosci.* **7**, 542–548.
48. Grossman, E. D. & Blake, R. (2002) *Neuron* **35**, 1167–1175.